Anal. Chem. **1998,** *70,* 2409−2414

Fast Aerosol Analysis by Fourier Transform Imaging Fluorescence Microscopy

Michal Fisher, Valery Bulatov, Salah Hasson, and Israel Schechter*

Department of Chemistry, Technion—Israel Institute of Technology, Haifa 32000, Israel

Fourier transform imaging spectroscopy was combined with fluorescence microscopy and a cooled CCD detector for fast analysis of aerosols contaminated with polycyclic aromatic hydrocarbons (PAHs). Aerosols were collected on glass fiber filters and inspected, for the first time, by this imaging technique, which provides a full fluorescence spectrum at each pixel. Mapping of PAH contamination was carried out and used for identification and quantification of the compounds. Quantification limits (based on 95% confidence intervals of calibration plots) in the 10 ng cm^{-2} range on filter are reported, which corresponds to 20 ng m^{-3} in air, integrated in 1 min. The absolute detection limit (on filter) is estimated as low as 0.25 pg, corresponding to an air concentration of 0.5 pg m^{-3}, integrated in 1 min. The method is examined for analysis of monocomponent contamination and for simple mixtures. After a proper automation, this method has the potential to provide in situ and on-line results regarding particulate airborne PAH contaminations.

Analyses of polycyclic aromatic hydrocarbon (PAH)-contaminated aerosols are of considerable industrial and environmental importance. These compounds, many of them known as carcinogenic or mutagenic agents, have to be monitored in air at workplaces and other public environments and are restricted to low concentrations by environmental regulations. Fast analysis of PAHs is also of importance for industrial process control. It is known that PAHs are formed by pyrolysis of carbonaceous materials at moderate temperatures or during oxidant-deficient combustion processes. Due to the low vapor pressure of many of these compounds, they are most likely to be found in aerosols or condensed onto aerosol particles.[1] Therefore, fast analysis of PAH aerosols is of current interest.

Despite the environmental and industrial needs, the problem of fast analysis of particulate airborne PAHs is not yet solved. Ambient aerosol particles are usually collected over an extended period, and the bulk samples are then characterized by conventional analytical techniques. Commonly used methods involve chromatographic separation followed by mass or optical spectrometric detection. GC/MS is used for the low-mass PAH compounds, while HPLC−MS is applied for the high masses.[2] These methods require volatility and solubility of the examined compounds in the mobile phase, respectively. The spectroscopic detection methods include UV absorption and luminescence measurements.[3] These conventional techniques usually provide accurate results; however, they are expensive and time-consuming. Interpretation of data is not simple and often requires experts.

Other important analytical techniques for PAH analysis include characterization of single aerosol particles by laser desorption/ionization (LDI) coupled with time-of-flight mass spectroscopy.[4,5] This method offers high sensitivity; however, the resulting calibration and quantification are rather complicated. Another method that provides integrated information on PAH contents in aerosols is based on the electron emission of these compounds.[6] This method is fast and provides direct results, but it has no particular selectivity, and it provides only a first indication of possible PAH contamination.

Most PAH compounds emit characteristic fluorescence spectra when irradiated with UV light. Fluorescence analysis in solutions is a simple and sensitive method for PAHs, where a common laboratory procedure includes an extraction of these compounds into a solvent and measurement of the fluorescence spectrum. Since many of these compounds emit also in the condensed form, direct fluorescence spectra can be obtained from solid aerosols as well.[7−9] This would be an advantage because it prevents errors which can be introduced by possible contamination during the extraction process.

Such direct applications are not practical, due to the low fluorescence intensities and the problems caused by PAH mixtures when light is integrated (over space and/or wavelengths) onto a detector. Thus, observation of the solid aerosols through a microscope may solve some of the problems. Fluorescence characteristics of some PAH microcrystals and their size dependence have been recently investigated.[10,11] In fact, the thermodynamic tendency helps in condensing relatively pure microscopic particulates. In this case, each microscopic particle consists of a single component (or of a simple mixture), while the bulk consists

(1) Lane, D. A. In *Organic chemistry of the atmosphere*; Hansen, L. D., Eatough, D. J., Eds.; CRC Press, Inc.: Boca Raton, FL, 1991; pp 155−198.
(2) Fetzer, J. C. In *Chemical Analysis of polycyclic aromatic compounds*; Vo-Dinh, T., Ed.; John Wiley & Sons: New York, 1988; pp 59−101.
(3) Zander, M. In *Chemical Analysis of polycyclic aromatic compounds*; Vo-Dinh, T., Ed.; John Wiley & Sons: New York, 1988; pp 171−196.
(4) Johnston, M. V.; Wexler, A. S. *Anal. Chem.* **1995**, *67*, 721A−726A.
(5) Murphy, D. M.; Thomson, D. S. *Aerosol Sci. and Technol.* **1995**, *22*, 237−249.
(6) Niessner, R.; Wilbring, P. *Anal. Chem.* **1989**, *61*, 708−714.
(7) Stevense, B. *Spectrochim. Acta* **1962**, *18*, 439−448.
(8) Birks, J. B.; Wright, G. T. *Proc. Phys. Soc.* **1954**, *67B*, 657−663.
(9) Birks, J. B.; Cameron, J. W. *Proc. R. Soc.* **1959**, *249A*, 297−317.
(10) Kasai, H.; Kamatani, H.; Okada, S.; Oikawa, H.; Matsuda, H. *Jpn. J. Appl. Phys.* **1996**, *35*, L221−L223.
(11) Tamai, N.; Porter, C. F.; Masahura, H. *Chem. Phys. Lett.* **1993**, *211*, 364−370.

S0003-2700(97)01355-3 CCC: $15.00
Published on Web 05/01/1998

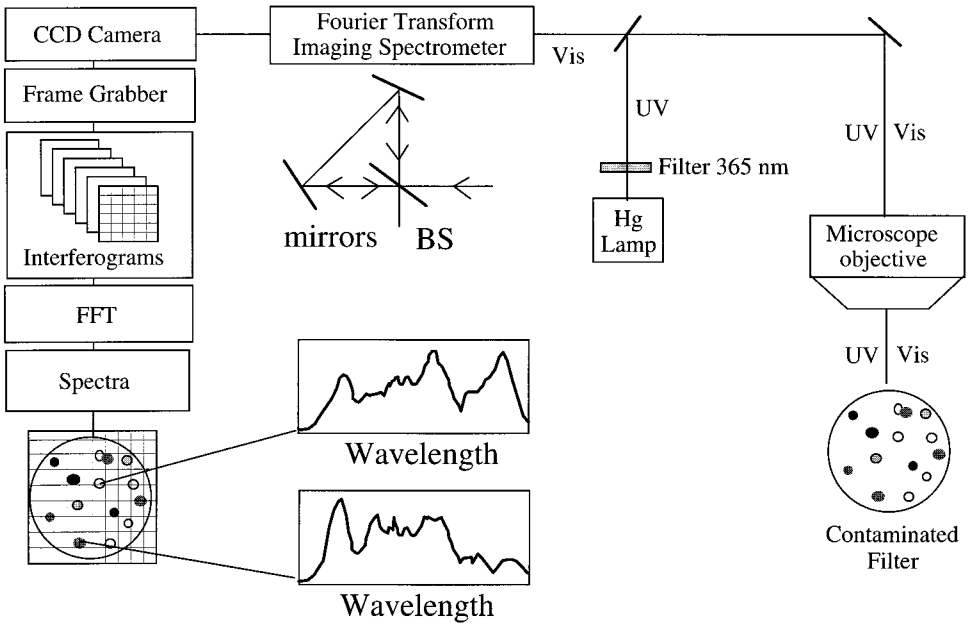

Figure 1. Schematic experimental setup for microscopic Fourier transform spectral imaging.

of a too-complicated mixture. Thus, microscopic fluorescence has a clear advantage over bulk observation.

Nevertheless, spatial resolution obtained by microscopes is not commonly coupled with spectral resolution, especially when visible fluorescence in concerned. Several imaging methods, coupled with a certain level of spectral information, have been recently investigated. Most methods are applied for Raman analysis;[12−16] however, fluorescence imaging was developed as well.[17−19] Most fluorescence imaging techniques are based on application of optical filters and provide limited spectral information, which is not sufficient for compound identification in mixtures. To solve this problem and to obtain both spatial and spectral resolutions, a new Fourier transform imaging spectrometer was coupled with a microscope and a CCD camera. This imaging instrument, which provides the fluorescence spectrum at each pixel, was applied for the first time for fast analysis of PAH aerosols.

This approach is also supported by morphological studies of aerosol particles, which indicate the possibility of source identification on the basis of aerosol characteristics.[20] The proposed setup provides both chemical and morphological information, which can be used for studying such source correlations.

EXPERIMENTAL SECTION

Sample Preparation. PAH aerosols were produced by an atomizing aerosol generator. PAH solutions in acetone (200 ppm) were atomized using a stable flow of nitrogen (99.999%). The resulting aerosol particles were carried along a 1-m glass tube fitted with dry air inlets. The liquid microdroplets were dried during this process such that, at the output, only the solid aerosol particulate cores were left.

Two PAH compounds were used for aerosol generation: perylene and sublimated coronene (Aldrich, 99%, no additional purification was carried out).

The aerosols were sampled onto glass fiber filters (Staplex TFAGF41), 1.2 cm diameter. Sampling was carried out by exposing the filters to the aerosol flow for predefined periods. No systematic aerosol generation or sampling was attempted, since an independent reference analysis procedure was carried out. Thus, the resulting PAH contamination was independently found, regardless of the details of the sample preparation procedure.

Experimental Setup. A special instrumental setup was constructed for PAH aerosol analysis, as described in Figure 1 and discussed in the following. The contaminated filters were examined by a UV fluorescence microscope coupled to a spectral imaging unit and a CCD camera. The microscope (Axiolab ABO100W/2, Carl Zeiss, Jena, Germany) was equipped with UV-transparent objectives (Fluar and Ultrafuar), providing several magnifications (×10, ×20, and ×40). Samples were irradiated by a mercury lamp, through the microscope objectives. PAH fluorescence was excited at 365 nm using a narrow-band filter (10 nm). A dichroic mirror placed in the optical path was used for cutting off the reflected light at wavelengths below 390 nm.

Microscope images were transferred to an imaging Fourier transform spectrometer and to a CCD camera (FIPA 20, Green Vision Systems, Israel) for simultaneous recording of the fluorescence spectra at each image pixel. The electrothermaly cooled CCD detector consisted of 480 × 640 pixels of 10 × 10 μm^2 each (Hamamatzu 4880).

Data Analysis. The data analysis program was written in C++ language, compiled and run on a PC (Pentium 166-MHz processor) under Windows NT operating system.

(12) Brenan, C. J. H.; Hunter, I. W.; Brenan, J. M. *Anal. Chem.* **1997**, *69*, 45−50.
(13) Morris, H. R.; Hoit, C. C.; Miller, P.; Treado, P. J. *Appl. Spectrosc.* **1996**, *50*, 805−811.
(14) Markwort, L.; Kip, B.; Da Silva, E.; Roussel, B. *Appl. Spectrosc.* **1995**, *49*, 1411−1430.
(15) Schaeberle, M. D.; Kalasinsky, V. F.; Luke, J. L.; Lewis, E. N.; Levin, I. W.; Treado, P. J. *Anal. Chem.* **1996**, *68*, 1829−1833.
(16) Zhao, J,; McCreery, R. L. *Appl. Spectrosc.* **1996**, *50*, 1209−1214.
(17) Vitt, J. E.; Engstrom, R. C. *Anal. Chem.* **1997**, *69*, 1070−1076.
(18) Panova, A. A.; Pantano, P.; Walt, D. R. *Anal. Chem.* **1997**, *69*, 1635−1641.
(19) Nomura, S.; Nakao, M.; Nakanishi, T.; Takamatsu, S.; Tomita, K. *Anal. Chem.* **1997**, *69*, 977−981.
(20) Reist, P. C. *Introduction to aerosol science*; Macmillan Publishing Co.: New York, 1984.

Reference Analysis. Each contaminated filter examined was divided into several parts. One was used for imaging fluorescence analysis, while the rest were analyzed by the reference standard method. Each sample was extracted with 3 mL of acetonitrile (Bio-Lab Ltd., Jerusalem, Israel). PAH analysis was performed using a fluorometer (Perkin-Elmer 50) calibrated with standard PAH solutions in the same concentration range as the examined samples.

RESULTS AND DISCUSSION

2D Spectral Imaging. Spectral imaging was achieved by combining imaging optics, a Sagnac interferometer, and an imaging detector, as schematically shown in Figure 1. The principle of operation is that the full optical image of the examined object (the contaminated filter in our case) is transferred to the interferometer, resulting in a large sequence of imaging interferograms. These interferograms are CCD images obtained when the true object image is split and recombined (after a certain optical retardation). The final 2D spectral information is then achieved by application of fast Fourier transform (FFT) at each pixel of the CCD detector.

In our interferometer, the two split coherent imaging beams travel a common path in opposite directions. This feature contributes to the intrinsic stability of the instrument. The optical path difference results from the angular rotation of the mirror.

It should be noted that this procedure ends up with full fluorescence spectra at each pixel of the inspected object, thus allowing for simultaneous morphological and chemical (spectral) analysis. This setup is advantageous over other methods providing similar results (e.g., acousto-optical tunable filters (AOTF)[21−25] and liquid-crystal tunable filters (LCTF)[13,22,26]), due to its much higher light throughput. The Sagnac interferometer has moving parts which are not desirable in field applications; however, its light-common-path design ensures high stability: small variations in the optical components affect both beams and do not alter the spectral measurement. Moreover, the temperature sensitivity of our method is low, which makes it a suitable technique for in situ applications.

Data Analysis. The data analysis program consists of several subunits. First, the spectrum at each pixel is constructed by FFT applied to the interferogram set. Then, the spectrum at each pixel is compared to a database of reference spectra for compound identification and for 2D chemical mapping. Both the fluorescence intensity and the spectrum are considered in the chemical mapping, as described in the following. The final quantification is based on the *fluorescence volume*, defined as the product of the emitted intensity and the number of pixels possessing the spectrum of the analyzed compound.

Since each CCD image represented an area of only ∼100 μm^2, several (∼20) images were examined for an appropriate statistical sampling of the contaminated filter. Results could be further improved by more extensive sampling; however, the currently used manual sampling method was too time-consuming. An automated sampling hardware is under development, such that numerous sampling sites can be handled. This is of considerable importance when the contamination is not homogeneously distributed on the filter or when complicated samples, requiring improved signal-to-noise ratio by statistical integration, are considered.

After spectral construction at each pixel, the so-called *emitters* are identified. Emitters are sets of connected pixels possessing an integrated intensity above a certain predefined threshold value.

Classification and Quantification. All emitters were noted and characterized by the following classification and quantification procedures. Classification was first carried out by a mapping algorithm used for mapping several components on the same sample. It performs classification by the highest degree of similarity to reference spectra. The difference between the spectrum of each pixel and that of each reference spectrum in the reference set is calculated. The difference between the spectrum $S_{xy}(\lambda)$ at pixel $\{x,y\}$ and the n reference spectra R_1, R_2, ..., R_n is given by

$$D_i = \sqrt{\sum_{\lambda}[S_{x,y}(\lambda) - R_i(\lambda)]^2}$$

This information was used for the assignment of each pixel and for presentation in "chemical maps" of the sampled filter. The classification threshold used for the above pixel assignment was varied until best results were obtained. A 20% similarity to a reference spectrum was found to be a reasonable classification threshold.

This approach has three main advantages over data acquisition using dielectric filters corresponding to the expected emission maxima: First, the light throughput is much higher in our case, since the whole visible spectrum is transferred, resulting in a better sensitivity. Second, the full fluorescence spectrum is utilized for compound identification. Therefore, a correct quantification is possible even when partially overlapped spectra are faced. Third, our approach can handle unknown substances on the filter, which can be identified and quantified from their fluorescence spectra.

Examples of two reference spectra (R_i) of PAH compounds used in this study are shown in Figure 2. These spectra were taken from solid aerosols of the pure compounds. Solid-state fluorescence spectra of particulate materials are somewhat different from the well-known solution figures; thus, a database of PAH aerosol spectra has to be compiled.

An example of 2D wavelength-integrated imaging of the fluorescence, obtained from a 49 416 μm^2 filter area (213 × 232 μm^2), is shown in Figure 3. The peaks represent the emitting contaminating aerosols, while the contour map at the bottom indicates their precise location and size. This figure was obtained from a glass filter containing a mixture of PAH-contaminated aerosols. These fluorescence intensities are integrated over all wavelengths.

(21) Schaeberle, M. D.; Karakatsanis, C. G.; Lau, C. J.; Treado, P. J. *Anal. Chem.* **1995**, *67*, 4316.

(22) Wang, X.; Lewis, E. N. Acousto-Optic Tunable Filters (AOTF) and their Application in Spectroscopic Imaging and Microscopy. *Fluorescence imaging spectroscopy and microscopy;* John Wiley & Sons: New York, 1996.

(23) Treado, P. J.; Levin, I. W.; Lewis, E. N. *Appl. Spectrosc.* **1992**, *46*, 553.

(24) Treado, P. J.; Levin, I. W.; Lewis, E. N. *Appl. Spectrosc.* **1992**, *46*, 1211.

(25) Goldstein, S.; Kidder, L.; Herne, T.; Levin, I. W.; Lewis, E. N. *J. Microsc.* **1996**, *184*, 35.

(26) Wodnicki, P.; Lockett, S.; Pillai, M. R.; McKalip, A.; Herman, B. In *Fluorescence imaging spectroscopy and microscopy;* Wang, X. F., Herman, B., Eds.; John Wiley & Sons: New York, 1996, pp 31−53.

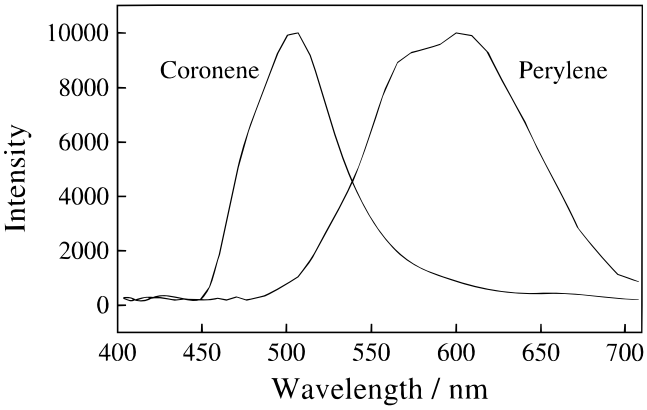

Figure 2. Condensed-state fluorescence spectra of perylene and coronene aerosols, recorded using the imaging fluorescence microscopy technique.

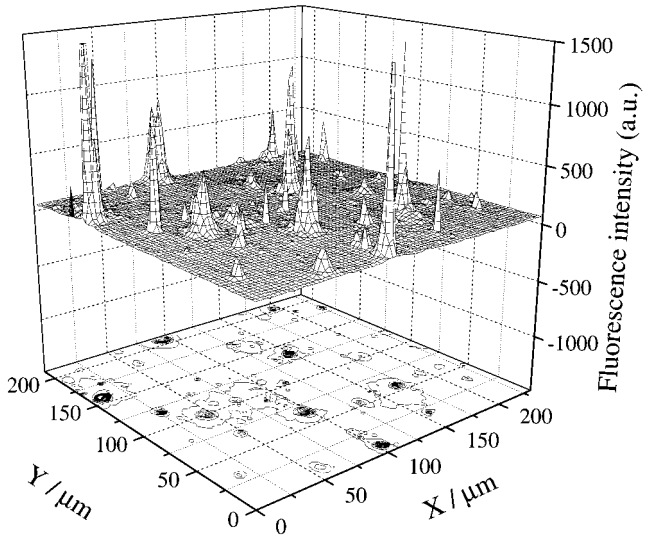

Figure 3. 2D wavelength-integrated fluorescence imaging map, obtained from a contaminated filter area of 213 × 232 μm^2. Fluorescence intensities of emitting aerosols are shown together with the contour map.

Application of the classification algorithm to the above sample provides a 2D mapping of the contamination, as shown in Figure 4. The dark gray pixels represent perylene contamination, while the light gray ones represent coronene. Each spot on this figure corresponds to a particular peak in the previous one; however, here we already have the chemical speciation. As can be seen, some of the peaks correspond to local mixtures of the PAH compounds involved, and this information can only be revealed using the classification technique.

Quantification of the two PAH components was based on the *volume* (*V*), obtained as a product of the number of pixels (area, *A*) and their corresponding emission intensity, for each compound (I_{xy}), given by

$$V = \int I_{x,y}\, dA$$

The current software improves quantification by considering a possible PAH mixture in each pixel. The spectrum there is fitted by a linear combination of the suspected spectra, and the contribution of each compound is obtained by the fitting parameters. (For the sake of the simplicity of presentation, only the major component at each pixel is shown in our figures.)

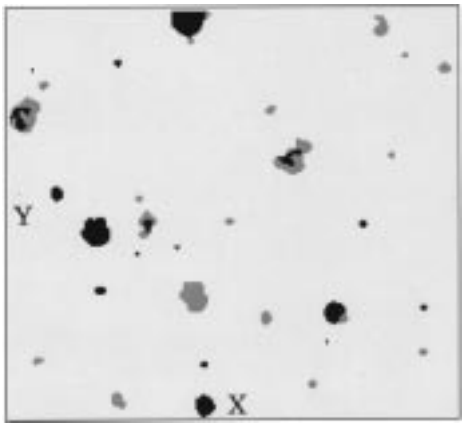

Figure 4. 2D classification map obtained from the contaminated filter shown in Figure 3. The dark and light gray pixels represent perylene and coronene aerosols, respectively.

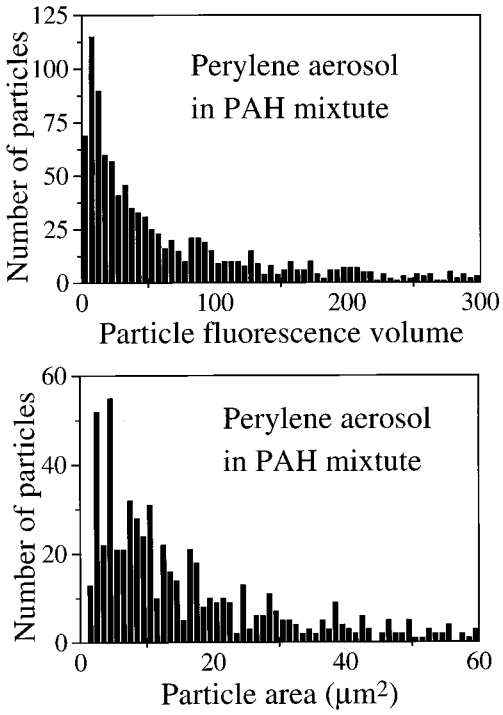

Figure 5. Distribution of perylene aerosols area (bottom) and their fluorescence volume (top).

An even better quantification procedure, now under development, is based on application of multivariate methods, such as principal component regression and partial least squares. These methods were not needed for analysis of simple aerosol mixtures as studied here; however, they become indispensable when real ambient contaminations are to be considered.

Size Distribution. Distributions of emitters' size (area) and fluorescence volume were obtained at each examined location. Such distributions for perylene aerosols (averaged over ~60 samples) are shown in Figure 5. In this case, most particle sizes were counted in the 4−5 μm^2 bin, and a similar distribution is observed for the fluorescence volumes. These features depend on the aerosol generation procedure.

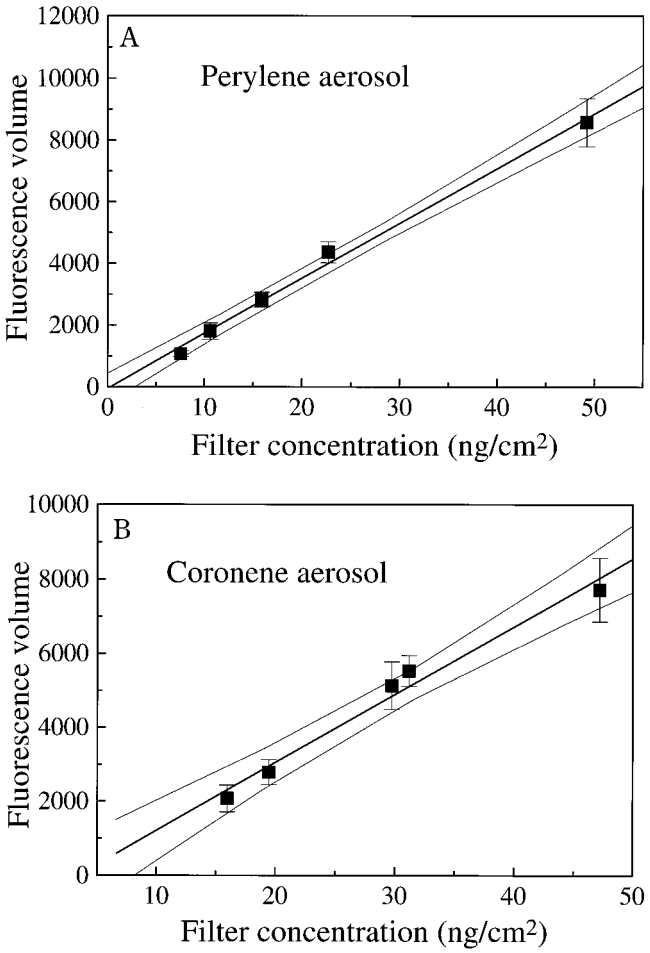

Figure 6. Total fluorescence volume of (a) perylene and (b) coronene obtained from monocomponent contaminated filters vs filter concentrations (analyzed by the reference method).

When studying the low-range detection limits, the instrumental parameters were varied such that smaller aerosols were generated. It should be noted that the smallest bin is defined by the pixel size at each particular magnification. In most cases, each pixel represents an rectangular area of 1 μm^2. Thus, smaller particles cannot be sized correctly, although they are accounted for, due to their fluorescence light emission.

The smaller particles are clearly observed with our optical method, however, at a resolution limited size of $\sim$1 μm^2. Nevertheless, the PAH quantification is still correct, since our procedure counts the fluorescence *volume*, which is affected only by the photon flux and does not suffer from the spatial resolution limitation.

Analysis of Monocomponent PAH Aerosols. The above-described procedures were applied for analysis of perylene- and coronene-contaminated aerosols (separately). The calibration plots (based on the emission volume) are shown in Figure 6. The 95% confidence interval LOD was 5 ng cm^{-2} for pyrene and 8 ng cm^{-2} for coronene. More interesting are the results related to the detection limits of these compounds in air. At an air sampling rate of 5 m^3 $min.^{-1}$, such as of a typical high volume sampler, operated for 1 min, the resulted detection limits are about 20 ng m^{-3} for these compounds.

Analysis of PAH Mixtures. Mixtures of perylene and coronene aerosols were prepared and sampled on glass fiber filters, using the same procedures. The classification and quantification algorithms were applied for analysis of the two components in the mixture, and calibration plots were obtained.

These plots are still linear in the examined range but somewhat worse than those obtained for monocomponent contamination. The reason is probably that the simple classification algorithm currently applied cannot handle correctly the spectra from pixels where both compounds are present. The composed spectrum is too different from the references and, thus, is rejected. A better algorithm, using multivariate analysis, is under development. The currently obtained 95% confidence interval-based LODs are 8 and 14 ng cm^{-2} for pyrene and coronene in PAH mixtures (correspondingly).

It should be noted that, in this case, the spectral imaging analysis is much simpler than the traditional methods based on PAH extraction. The latter actually mixes up the compounds that are well separated on the filter (due to their very nature). Moreover, the extraction procedure involves dilution of the PAH compounds, while the proposed method takes advantage of the high local concentration on the filter.

There are several problems that limit the performance of this method. One of the severe problems is related to the flatness of the examined filter. Actually, the filters are not flat on the microscopic level. Therefore, refocusing is required at each examined site. However, when the smallest aerosol particulates are considered, a common focusing condition cannot be estab-

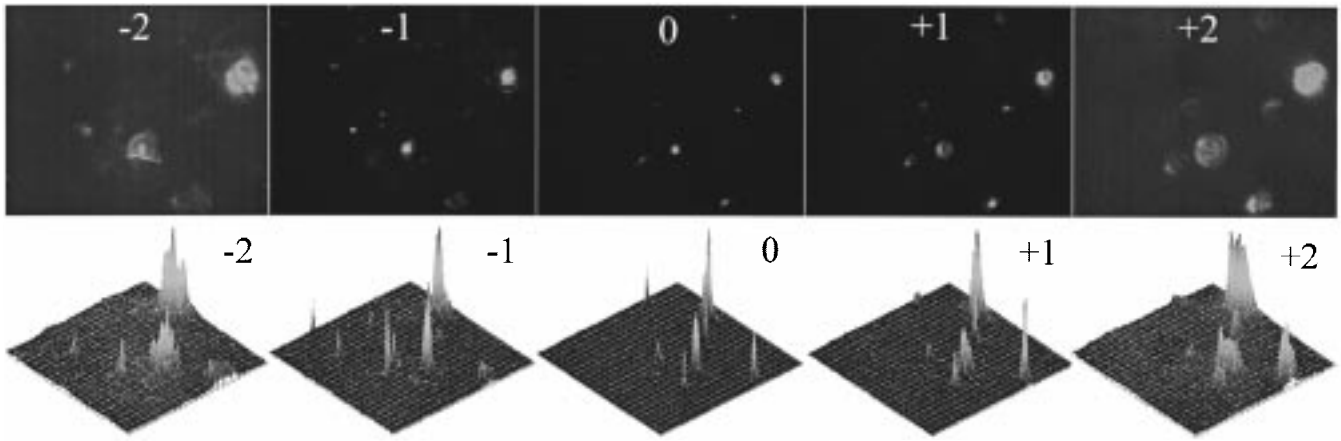

Figure 7. Wavelength-integrated fluorescence imaging of a PAH-contaminated filter at several microscope focusing conditions (top), together with their corresponding 3D representation (bottom).

lished, even for one microscopic scene. This problem is illustrated in Figure 7, where microscopic fluorescence images of the same site are presented at five different optical focusing conditions. In the center image, the central aerosol particle is just in focus, while the other images, to the left and to the right, correspond to out-of-focus conditions in both directions. It can be seen that the size of some emitters changes. This, by itself, is not a severe problem for PAH quantification, since the fluorescence *volume* is not changed. As the particles seems larger, the intensity is reduced correspondingly. However, at a certain limit, the emitted light per pixel becomes comparable to the background noise, and in this case information is lost. Moreover, a detailed observation of these figures reveals that, at each focusing condition, some new emitters appear, while others disappear. This is a result of the unflatness of the filter surface within a single microscopic scene. A possible solution to this issue (which is now under investigation) is based on automatic measurement of each image at a series of focusing conditions. Then, chemometric algorithms can be applied for correction of the image and bringing each emitter (particle) into focus.

Absolute Detection Limits. The absolute detection limits of this method are determined by the mass of a single particulate aerosol observed and identified on the collection filter. We observed extremely small particulates on the filter; however, it seems that the estimation of the size (and then the mass) of such particulates is limited by the diffraction limit, which for most emitted light is of the order of 700 nm (using an objective of NA = 0.5). Based on these figures, we estimated the absolute limit of detection as 0.25 pg. Further experiments, with smaller aerosol particles and longer detector integration times, are planned and might reduce this result.

CONCLUSIONS

A method for fast-aerosol analysis is suggested, based on chemical imaging of aerosol-contaminated filters with microscopic and spectral resolutions. The current results indicate the feasibility of this method (and by no means constitute a complete method establishment). The 95% confidence interval LODs reported here are in the 10 ng cm^{-2} range but can be further improved by a more extensive sampling program. The calculated LOD, based on detection of a diffraction-limited particle size, is ~0.25 pg. When actually detected particles of 0.2-μm size (diameter) are considered, the resulted detection limits are as low as 6 fg. Better results can be obtained using a liquid nitrogen-cooled CCD detector, since much smaller particles can still be observed in the time-integrated mode (although the spatial resolution will not be better).

Analyses of simple aerosol mixtures were shown. Linear calibration plots were obtained in this case as well, although the resulting correlation coefficients were somewhat lower. Further research on more realistic mixtures is under investigation.

The suggested method provides both morphological and chemical information on PAH aerosols. This combination may be used in the future for pollution source identification, since it is expected that each main source has its characteristic emission fingerprint regarding the chemical composition and morphological pattern of individual particulates.

ACKNOWLEDGMENT

Collaboration with D. Moshe and N. Horesh of Green Vision Systems Ltd. is much appreciated. This research was supported, in part, by Green Vision Systems Ltd. (Israel) and by the James Franck Program in Laser Matter Interaction.

Received for review December 16, 1997. Accepted March 6, 1998.

AC971355C